ISJ 23: 10-23, 2026 ISSN 1824-307X

RESEARCH REPORT

Identification and characterization of a pathogenic *Vibrio parahaemolyticus* causing translucent post-larvae disease in *Penaeus vannamei*

R Fan[1,2], T Chen[1,2], M-Q Wang[1,2,3,4,5*]

[1]MOE Key Laboratory of Marine Genetics and Breeding, (Shandong Key Laboratory of Marine Seed Industry), College of Marine Life Science, Ocean University of China, Qingdao 266003, China
[2]Hainan Key Laboratory of Tropical Aquatic Germplasm (Hainan Seed Industry Laboratory), Sanya Oceanographic Institution, Ocean University of China, Sanya 572024, China
[3]Hebei Xinhai Aquatic Biotechnology Company Limited, Cangzhou 061100, China
[4]Hainan Lanyin Aquatic Breeding Technology Company Limited, Wenchang 571343, China
[5]Qingdao Institute of Blue Seed Industry (Shandong Engineering Research Center of Blue Seed Industry), Qingdao 266071, China

 Accepted February 12, 2026

Abstract

Penaeus vannamei is an important aquaculture species, but disease outbreaks posed a serious threat to the sustainable development of shrimp farming. In recent years, a fatal disease known as translucent post-larvae disease (TPD) has emerged in many farms, characterized by the vacuolization of the hepatopancreas and the pallor or colorlessness of the intestine. In this study, we obtained a strain of *Vibrio parahaemolyticus*, named H1, that could cause TPD in both juvenile and adult shrimps. *V. parahaemolyticus* H1 could cause gradual atrophy of the hepatopancreas, deepening of the intracellular material color, and eventually complete vacuolization. Antibiotic susceptibility tests revealed that *V. parahaemolyticus* H1 was resistant to chloramphenicol, ceftriaxone, and sulfamethoxazole trimethoprim, but exhibited resistance to tetracycline. The 2b-RAD-M analysis showed that *V. parahaemolyticus* H1 could disrupt the shrimp intestinal microbiota and lead to a loss of resistance to environmental bacteria. These results identified a pathogenic *V. parahaemolyticus* causing TPD from *P. vannamei*.

Key Words: *Vibrio parahaemolyticus*; translucent post-larvae disease; intestinal microbiota

Introduction

Penaeus vannamei is one of the most cultivated aquatic shrimps in the world, owing to its higher larval survival rate and its adaptability to various salinities (Sun *et al*., 2022). With the development of shrimp aquaculture, periodic outbreaks of infectious diseases have become more frequent. In addition to known pathogens, new pathogens are constantly emerging, causing large numbers of shrimp deaths and causing serious economic losses to farmers (Yang *et al*., 2022). Recently, a new type of disease called translucent post-larvae disease (TPD) has posed a huge threat to shrimp growth and survival (Jia *et al*., 2026). TPD occurred mainly when shrimp grew to 4-7 days old. Diseased shrimps exhibited similar clinical signs, such as the hepatopancreas becoming pale, the digestive tract emptying, which caused the infected shrimp body to become transparent and translucent (Zou *et al*., 2020). Large-scale mortality higher than 90% typically occurred within 24-48 h after the appearance of the first abnormal individuals (Yang *et al*., 2022).

Certain strains of *Vibrio parahaemolyticus* have been identified as the pathogen causing TPD (Broberg *et al*., 2011). *V. parahaemolyticus* is a gram-negative bacterium living in estuarine and marine environments and is known as an opportunistic pathogen whose pathogenicity is formed by the expression of a series of virulence factors (Ashrafudoulla *et al*., 2021). In general, virulence factors can infect and destroy the host, by allowing pathogenic adhesion and entry, establishing, and proliferating, avoiding host defenses, harming the host, and eventually leaving the infected host (Darshanee *et al*., 2012). Thermostable direct hemolysin (TDH) and TDH-related hemolysin (TRH) are the two main virulence factors of *V. parahaemolyticus* (Zhong *et al*., 2022). However, these factors were not found in the strains causing TPD in shrimps. Instead, a new virulence factor,

Corresponding author:
Mengqiang Wang
MOE Key Laboratory of Marine Genetics and Breeding
Shandong Key Laboratory of Marine Seed Industry
College of Marine Life Science
Ocean University of China
Qingdao 266003, China
E-mail: wangmengqiang@ouc.edu.cn

Table 1 Primers used in experiments

Name	Sequence
Tdh-R	TGGATAGAACCTTCATCTTCCACC
Tdh-F	GTAAAGGTCTCTGACTTTTGGAC
Trh-R	CATAACAAACATATGCCCATTTCCG
Trh-F	TTGGCTTCGATATTTTCAGTATCT
Tlh-R	GCTACTTTCTAGCATTTTCTCTGC
Tlh-F	AAAGCGGATTATGCAGAAGCACTG
PirAB-F	GGTGGACGTTAAACGGATACA
PirAB-R	CCTGTAGTACGGCGACATTAAG
PirAB-AF	GGATCCATGCAGTCAGCTATCAGCGAG
PirAB-AR	TCAAAGAATGTTGTTACTCTGGGTACC
27F	AGAGTTTGATCCTGGCTCAG
1492R	ACGGYTTACCTTTTTGCGG

Vibrio high virulent protein (VHVP), was identified (Mahoney *et al*., 2010). VHVP was encoded by three gene segments, which was located on the plasmids of the *Vibrio* genome, and played a key role in its pathogenicity (Mahoney *et al*., 2010). However, the pathogenic mechanism of *V. parahaemolyticus* causing TPD is still unclear.

The gut is the first site where bacteria enter the body. Intestinal microbes play an important role in regulating nutrient absorption, metabolic processes to promote host health (Wang *et al*., 2025). They also act as a barrier in the fight against pathogen invasion, and stimulate immune response through secreting extracellular products (Rooks and Garrett, 2016). The invasion of pathogenic bacteria can disrupt the stability of the host intestine (Shi *et al*, 2026). Ecological changes in the intestinal flora can also lead to the development of the disease (Han *et al*., 2025).

In this study, we isolated and identified a pathogenic strain of *V. parahaemolyticus*, named H1, which could cause TPD in both juvenile and adult shrimps. The basic characteristics of the *V. parahaemolyticus* H1 were systematically assessed, including Gram staining and scanning electron microscopy to observe its morphological features, as well as partial physiological and biochemical experiments to analyze its metabolic products. Tissues section analysis was conducted to observe the pathological changes in the hepatopancreas of shrimps caused by *V. parahaemolyticus* H1 infection. Furthermore, the study focused on investigating the impact of *V. parahaemolyticus* H1 infection on the composition of the shrimp intestinal microbiota and its potential effects on intestinal function.

Materials and methods

Samples collection

Healthy and diseased shrimps were collected from Hebei Xinhai Aquatic Biotechnology Co., Ltd. in Huanghua, China. The shrimp was placed in a sterile bag and transported to the laboratory using dry ice. After being shipped to the laboratory, the samples were thawed and washed three times with 75% ethanol, followed by washing with deionized water to remove environmental pollution, and then stored at -80 °C.

Strain purification

The diseased shrimp samples were transferred into 1.5 mL sterile centrifuge tubes, followed by the samples being cut into small pieces with scissors. An appropriate amount of the homogenized sample was then taken and inoculated onto 2216E agar medium. The inoculated plates were then incubated at 28 °C for 24 h. After incubation, we observe the bacterial colony morphology and select the most abundant and morphologically distinct colonies for further purification. The purified single colonies were then inoculated into 2216E liquid medium (HB0132-1, Hopebiol, China) and cultured in a shaking incubator at 28 °C for 24 h. The optical density (OD_{600}) of the bacterial suspension was measured using a spectrophotometer. When the OD_{600} reached 0.9 to 1.0, the bacterial concentration was approximately 10^8 to 10^9 CFU/mL, and the suspension were used for subsequent infection experiments.

Strain identification and sequence alignment

The genomic DNA of *V. parahaemolyticus* H1 was extracted using the Ezup Column Bacterial Genomic DNA Extraction Kit (B518255, Sangon, China), according to the manufacturer's instructions. The bacterial 16S rRNA gene was amplified by PCR using the universal primers, 27F and 1492R. The PCR products were purified, and sequenced on the ABI 3730 DNA sequencer. The sequence homology searches were performed in the National Center for Biotechnology Information (NCBI) database using the BLAST program. Phylogenetic tree was constructed by the neighbor-joining method in MEGA 11.0.11.

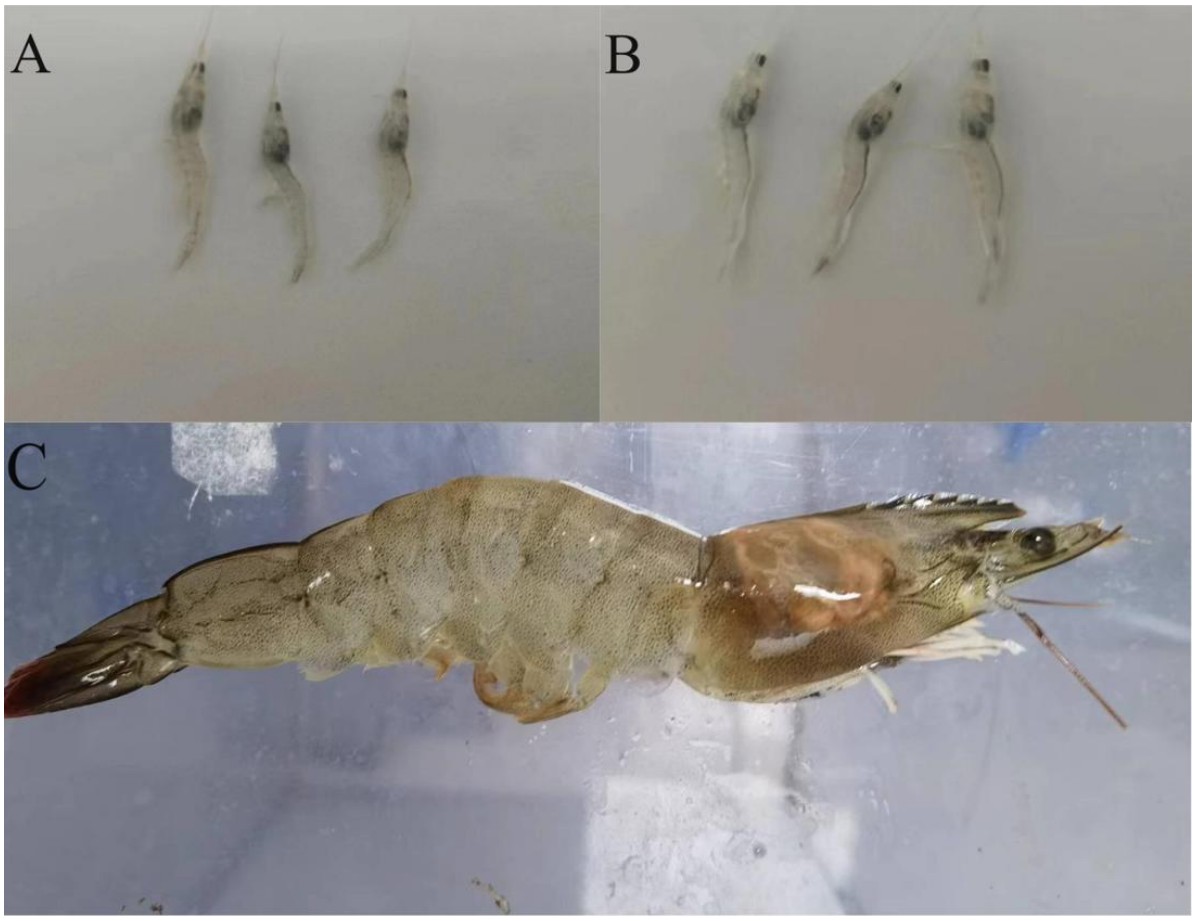

Fig. 1 Comparison of healthy and diseased shrimps. (A) healthy post-larva shrimps, (B) diseases post-larva shrimps, (C) adult diseased shrimps

Phenotypic analysis of V. parahaemolyticus H1

The EasyID Biochemical Identification Kit (HKI001, HKM, China) for *V. parahaemolyticus* H1 was used according to the instructions to assess the bacterial metabolic characteristics, fermentation ability, amino acid metabolism, and enzyme activity, aiding in bacterial classification and identification. To detect the presence of the virulence genes TDH, TRH, thermolabile hemolysin (TLH), *pir*A, and *pir*B in *V. parahaemolyticus* H1, specific primers were designed for PCR amplification (Table 1). Additionally, a commercial kit from Guangzhou Huafeng Biotechnology Co., Ltd. was used to test for the presence of the VHVP virulence factor.

For Gram staining and scanning electron microscopy (SEM) analysis, bacterial cultures were evenly spread onto glass slides and air-dried. The Gram staining procedures were as follows: first, the slide was stained with crystal violet for 1 min, then rinsed with PBS. Next, iodine solution was added for 1 min to fix the stain, followed by another PBS rinse. The slide was then decolorized with absolute ethanol for 30 s and counterstained with safranin for 1 min. Finally, it was rinsed with water, air-dried, and examined under a light microscope to observe bacterial morphology.

For SEM analysis, bacterial cultures were washed twice with PBS to remove any residual medium and then fixed in 2.5% glutaraldehyde solution. Then, the samples were stored at 4 °C and sequentially subjected to gradient ethanol dehydration, critical point drying, and gold sputter coating using a metal sputter coater. After these treatments, the samples were ready for SEM (S-3400N, Hitachi, Japan) observation.

Antibiotic susceptibility testing

Bacterial suspension was evenly spread on the surface of 2216E agar plates (HB0132, Hopebiol, China) to ensure uniform distribution. Then, antibiotic susceptibility test discs impregnated with different antibiotics were evenly placed on the surface of the agar plate using tweezers, ensuring full contact with the agar. Three identical antibiotic discs were placed on each plate, and the average result was taken for analysis. The inoculated plates were then inverted and incubated at 28 ℃ for 24 h. After incubation, the inhibition zones around each antibiotic disc were observed, and the diameters of the inhibition zones were measured using a ruler. Based on the size of the inhibition zones, the sensitivity of the bacteria to each antibiotic was determined.

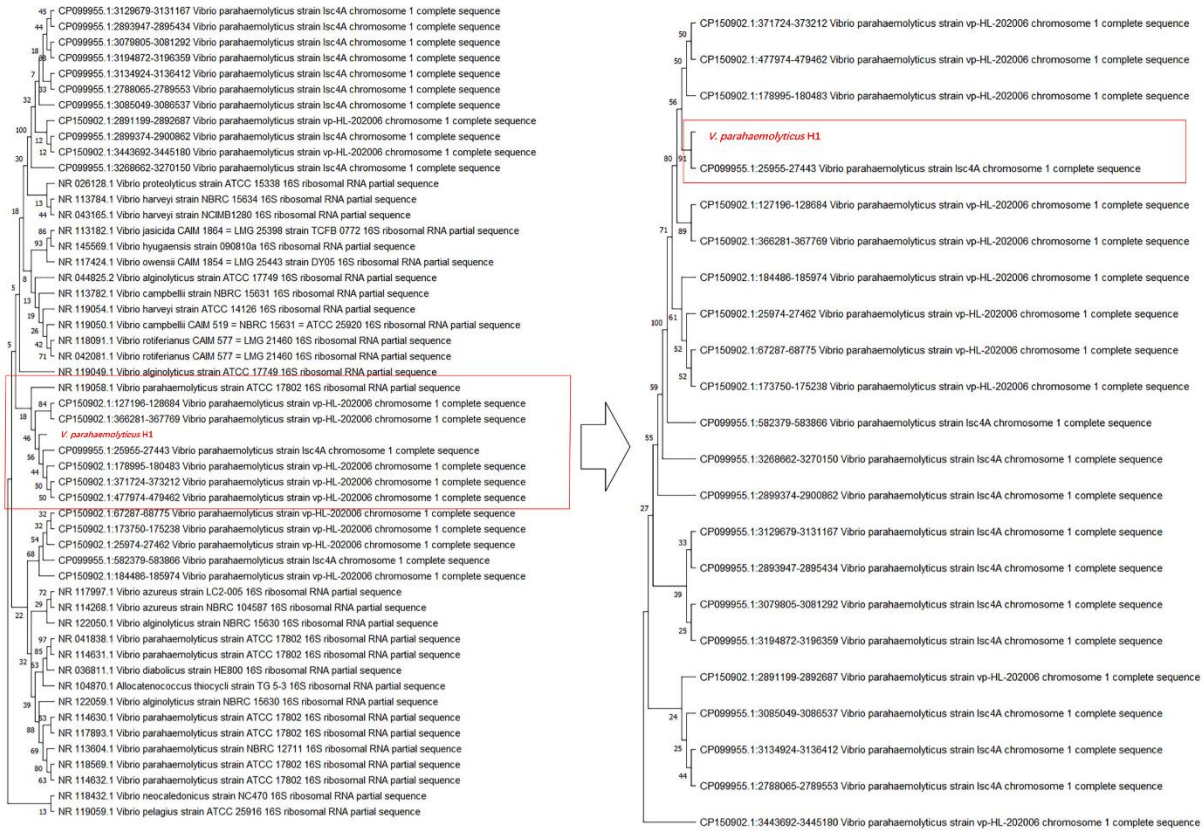

Fig. 2 Phylogenetic tree for *V. parahaemolyticus* H1 and twenty different *Vibrio* sequences derived from a conserved fragment of the 16S rDNA

Experimental challenges of shrimps with V. parahaemolyticus H1

In the challenge experiment, the average body length of juvenile shrimp was 10 ± 0.2 mm, and that of adult shrimp was 8 ± 2 cm. Juvenile shrimps were grouped at 50 individuals per tank, while adult shrimps were grouped at 10 individuals per tank, with a total of 12 tanks. The tanks were evenly divided into experimental and control groups, with 6 tanks in each group, consisting of 3 tanks for adult shrimp and 3 tanks for juvenile shrimp. Each tank was filled with 10 L of seawater and subjected to 24 h of starvation to ensure the intestines were empty. The shrimps in the control group received no treatment, while the shrimp in the experimental group were challenged by immersion in live bacteria at a final concentration of 1×10^6 CFU/mL. Mortality was observed every 2 h, and both the cumulative and average mortality rates was calculated at 24 h. As part of Koch's postulates, we performed bacterial isolation on dying shrimps.

Histopathology

In order to investigate the histological differences between the hepatopancreas of healthy and diseased shrimp, histopathological sectioning experiments were conducted. First, samples of healthy and diseased adult and juvenile shrimp were placed in a 4% paraformaldehyde (PFA) solution and soaked for 48 h for fixation. After fixation, the samples were dehydrated using a gradient ethanol solution, gradually increasing the ethanol concentration until the samples were fully dehydrated. The dehydrated samples were then immersed in paraffin and embedded in it. The paraffin-embedded tissue blocks were sectioned into approximately 5 μm thick slices and stained using the conventional Hematoxylin and Eosin (H&E) staining method (Ni *et al*., 2025). After staining, the sections were observed under a light microscope to analyze the histopathological characteristics of the hepatopancreas in both healthy and diseased shrimps.

Intestinal microbiota analysis

The homogenized and mixed shrimp gut samples were used for library construction (Hu *et al*., 2024). Briefly, DNA was extracted from the homogenate and digested with BcgI enzyme (R0545S, NEB, China) at 37 °C for 3 h. Then, adaptors were ligated to the DNA fragments. The ligation reaction was performed by mixing 5 μL of digested DNA with 10 μL of a ligation master mix containing T4 DNA ligase. The reaction was carried out at 4 °C for 12 h. After that, the ligation products were amplified, and the PCR products were loaded onto an 8% polyacrylamide gel. Bands of approximately 100 bp were excised from the gel and diffused in nuclease-free water for 12 h at 4 °C. The PCR products were purified using the QIAquick PCR

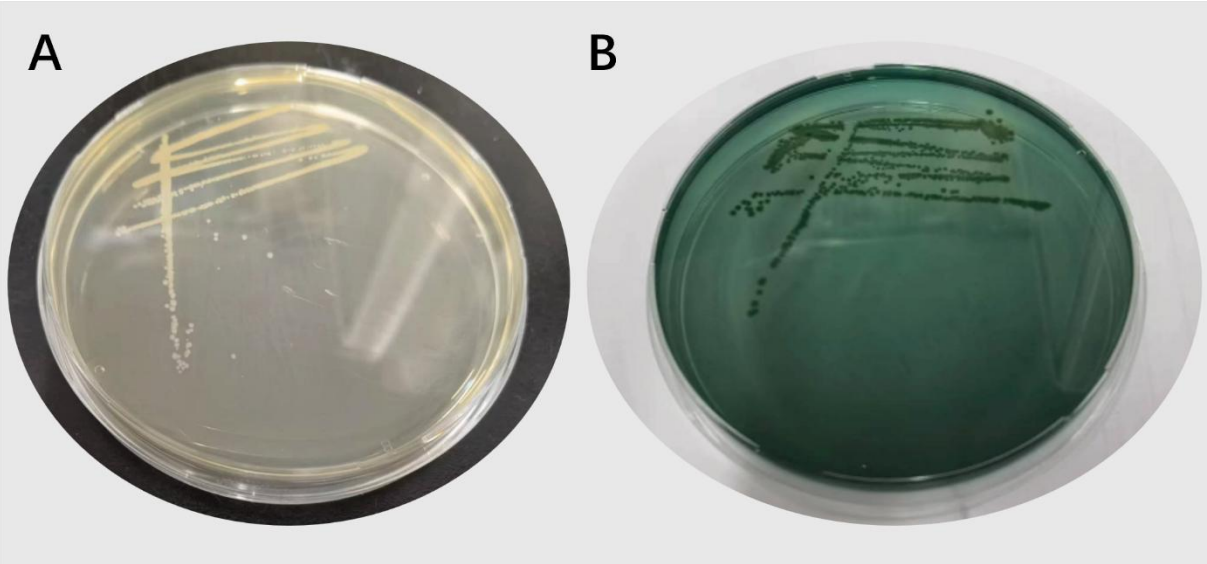

Fig. 3 Bacterial growth on TCBS and 2216E. (A) TCBS agar plates, (B) 2216E agar plates

Purification Kit (28106, Qiagen, Germany) and sequenced using the Illumina Nova PE150 platform.

Base recognition was performed from raw base data files obtained by high-throughput sequencing and the sequences containing digested fragments were extracted, and the reads containing more than 8% N bases were filtered and deleted, and the low-quality reads were filtered and deleted. Microbial annotation information for each clean reads was retrieved in the 2b-RAD-M database (Wang *et al*., 2026).

The possible microbial genomes were used for secondary library construction, and a Heatmap of the relative abundance level was established based on the species annotation information, and the species annotation results were visualized using Krona. The top 20 abundant species were selected, and the circlos plot was performed using the circlize package in R to reflect the proportion of each dominant species among different samples. Subsequently, the alpha-diversity, namely the Observer species index, the Shannon index, the Chao1 index, and the Simpson index, were calculated (Schloss *et al*., 2009).

In beta-diversity analysis, unweighted Unifrac distances were used to identify relationships between different samples based on bacterial community structure (Avershina *et al*., 2013), and the results were visualized and plotted by principal coordinate analysis (PCoA) (Caporaso *et al*., 2010). According to the t-test algorithm and Wilcoxon algorithm, the Heatmap plot was plotted according to the relative abundance of different species.

Linear discriminant analysis Effect Size (LEfSe) was used to identify statistically significant biomarkers in the samples, and the significance of their differences in intestine of healthy shrimp and diseased shrimp was compared. The correlation between species or environmental factors and species was also analyzed and calculated, and the obtained numerical matrix was visually displayed in the Heatmap. The function of the gut microbiota was predicted using the Kyoto Encyclopedia of Genes and Genomes (KEGG).

Statistical analysis

All experiments were performed in triplicate parallel experiments, and the results data were expressed as mean ± standard deviation (SD). Statistical analysis was performed using Minitab 19. The one-way analysis of variance (ANOVA) embedded in the software SPSS 13.0. $P < 0.05$ was considered statistically significant.

Results

Characteristics of diseased shrimps

Compared to the healthy animals (Fig. 1A), the clinical manifestations of diseased shrimp (Fig. 1B) were similar, with not eating, sluggish movement, pale or colorless hepatopancreas. A high percentage

Table 2 Effect of pH on bacterial growth

pH	OD_{600}
seawater	0.63730±0.01340
3	0.05267±0.00309
4	0.06977±0.00352
5	0.62010±0.03074
6	0.69220±0.02074
7	0.69210±0.01129
8	0.71530±0.01530
9	0.66970±0.01126
10	0.12140±0.01790

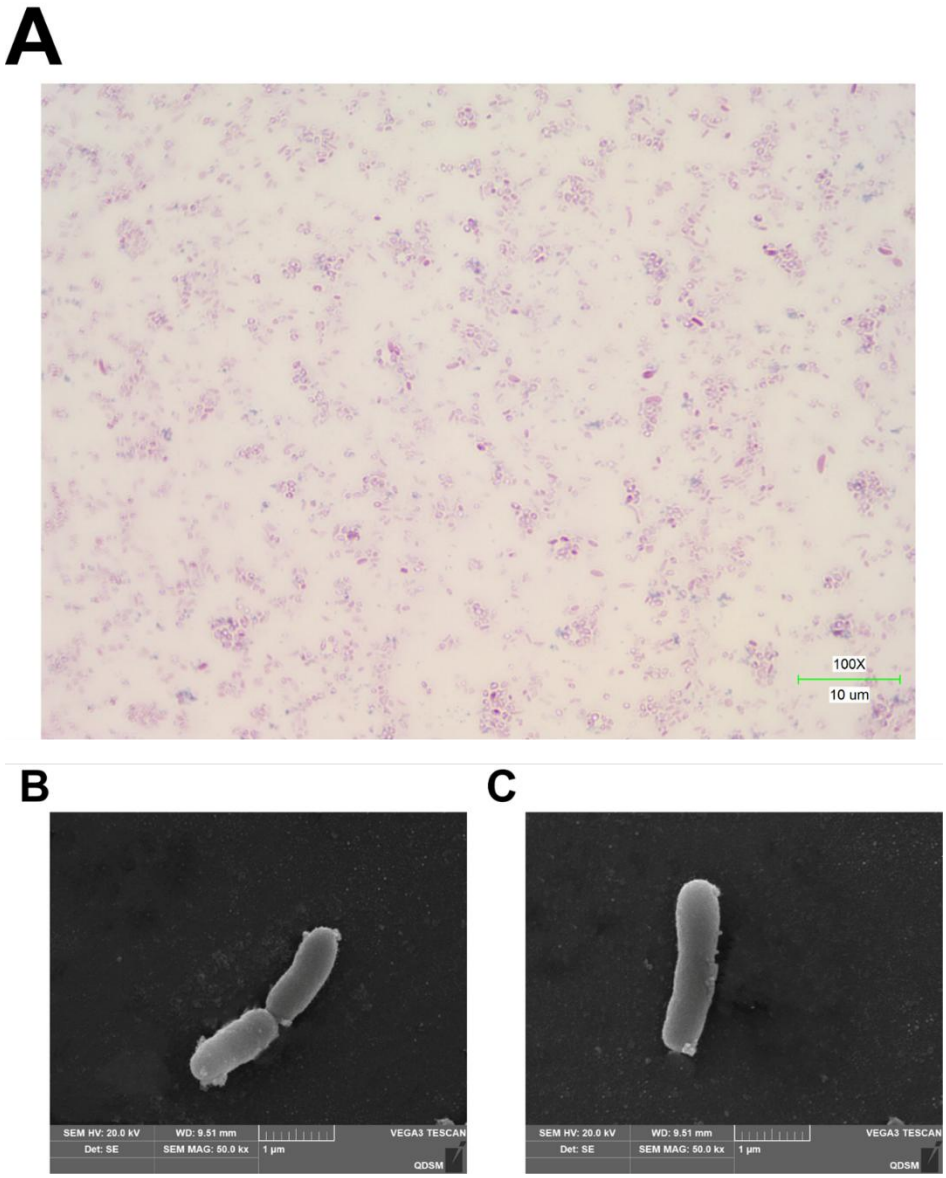

Fig.4 Bacterial morphology. (A) gram stain under light microscopy, (B) and (C) scanning electron microscope observation

of infected shrimp fry sunk to the bottom because of the invasion of bacteria, the ability to swim was reduced. We prepared juvenile shrimp and adult shrimp and conducted a challenge experiment on the strains we isolated from the farm, and found that the juvenile shrimp began to die from about 9 h, and the mortality rate was as high as 90% within 24 h. Interestingly, adult shrimp also began to die 16 h after challenge, and after 48 h, the mortality rate of adult shrimp also reached 90% (Fig. 1C). According to Koch's postulates, we first isolated *V. parahaemolyticus* H1 from diseased shrimp. Then, we inoculated this strain into healthy shrimp, and after 24 h of observation, clinical symptoms resembling natural infection appeared, such as sluggish movement and pale hepatopancreas. Subsequently, we re-isolated and identified the bacteria from the dead shrimp, and found that they were the same as the original strain, both being *V. parahaemolyticus*. Based on these results, we confirmed that this strain is pathogenic.

16S rDNA sequencing and phylogenetic analysis

The bacterial sequence was 1489 bp after 16S rDNA sequence analysis. PCR product sequences were analyzed by BLAST (Fig. 2). The strain showed a high degree of similarity with *V. parahaemolyticus* strain Isc4A chromosome 1 in the database. The phylogenetic tree was constructed by using neighbor-joining method and MEGA software, which further confirmed that the isolated strain was *V. parahaemolyticus.*

Bacterial isolation and culture

The *pir*AB virulence factor in the strain was detected and the results were negative. TDH and TRH were also not detected in the *V. parahaemolyticus* H1. The VHVP virulence factor was detected positive. The colony was yellow-colored round colonies on TCBS agar with neatly raised edges and 1.86 ± 0.44 mm in diameter after 24 h incubation at 28 °C (Fig. 3A), however the pale-colored round colonies (1.37 ± 0.2 mm in diameter) on marine 2216E agar after incubation for 24 h at 28 °C (Fig. 3B).

Bacterial growth and characterization

We explored the effect of pH on bacterial growth and the results are shown below. Strain was found to grow at pH 6-8 as the appropriate growth pH (Table 2). The best growth rate was found at pH 7. The bacteria were stained as Gram-negative strains by Gram staining, and the bacteria were stained red. Under a 100 × oil microscope the bacteria are observed to be spherical in shape (Fig. 4A). Under scanning electron microscopy, the strain appeared elliptical with a smooth surface. A microcapsule structure was visible on the cell surface, but no flagella structure was observed (Fig. 4B).

Analysis of the agar diffusion method for antibiotic susceptibility testing

In this agar diffusion method antibiotic susceptibility experiment. The measurements of the inhibition zone diameters are shown in Table 3. The above results indicate that chloramphenicol (C), ceftriaxone (CTR), and trimethoprim sulfamethoxazole (SXT) are effective antibiotics, while ciprofloxacin (CIP), erythromycin (E) and gentamicin (GEN) showed poor antibacterial effects.

Table 3 Diameter of inhibition zones of different antibiotics

Antibiotics	Inhibition zone diameter
Penicillin	0.00
Ampicillin	0.00
Ceftriaxone	0.71±0.0125
Gentamicin	0.29±0.0057
Tetracycline	0.00
Chloramphenicol	0.69±0.00446
Trimethoprim-Sulfamethoxazole	0.71±0.01250
Lincomycin	0.00
Ciprofloxacin	0.27±0.01710
Erythromycin	0.00

The remaining four antibiotics did not demonstrate any inhibitory effects. This outcome highlights the importance of selecting appropriate antibiotics in clinical treatment and provides a basis for further research.

Histopathology

Histopathological examination revealed that the hepatopancreas and intestinal contours of healthy juvenile and adult shrimp were well-defined, exhibiting normal histological features (Fig. 5A, B). However, histological examination of diseased juvenile shrimp showed that, after bacterial immersion, the hepatopancreas was damaged, and the contours were blurred (Fig. 5C). Necrosis of the midgut epithelial cells occurred, and they detached

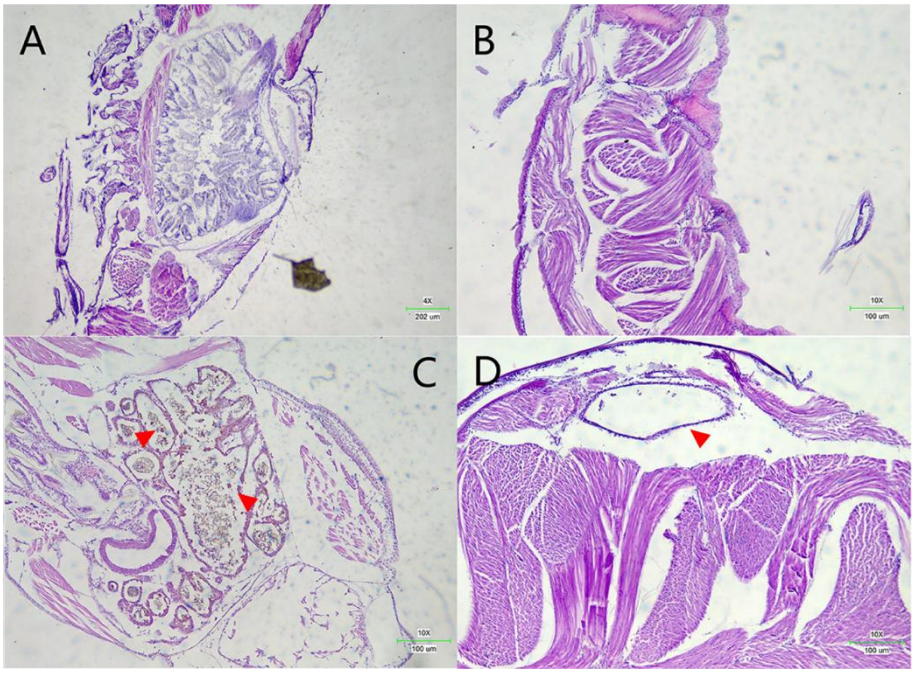

Fig. 5 Hepatopancreas changes in juvenile shrimp. (A) hepatopancreas of healthy shrimp, (B) healthy shrimp intestines, (C) hepatopancreas of diseased shrimp, (D) intestines of diseased shrimp

Fig 6 Hepatopancreas changes in adult shrimp. (A) healthy hepatopancreas of adult shrimps, (B) hepatopancreas of shrimp that survived after 6 h of pathogenic bacteria challenge, (C) hepatopancreas of shrimp that died after 18 h of pathogenic bacteria challenge

from the muscle cells, entering the intestinal tract. The intestinal wall was damaged, and the lumen was narrowed. Notably, bacterial colonization was also observed in the intestines of juvenile shrimp (Fig. 5D).

The mortality of adult shrimp after disease onset is relatively slow, so histopathological sections obtained at different time points allow for the observation of the continuous progression of the pathological process. In healthy shrimp, the hepatopancreatic cells are tightly connected. Over time, the cytoplasm of the hepatopancreas gradually atrophies, the color of the intracellular material deepens, gaps appear between the cells, and eventually, the contents of the hepatopancreas disappear, leaving the cells hollow (Fig. 6).

Changes in intestinal flora

The original sequence was stored in the NCBI sequence read archive (SRA) database with accession number PRJNA1045329. Compared with the control group, the values of observed species, Chao1, Simpson, and Shannon in the challenged group were higher, indicating that the strain destroyed the intestinal bacterial structure of shrimp and allowed bacteria in the environment to enter the intestinal tract of shrimp (Fig. 7A). According to the results of principal coordinate analysis (PCoA), the six samples were divided into two clusters, and the similarity analysis (ANOSIM) test showed that there were significant differences in the intestinal microbiota between the experimental group and the control group (Fig. 7B, C).

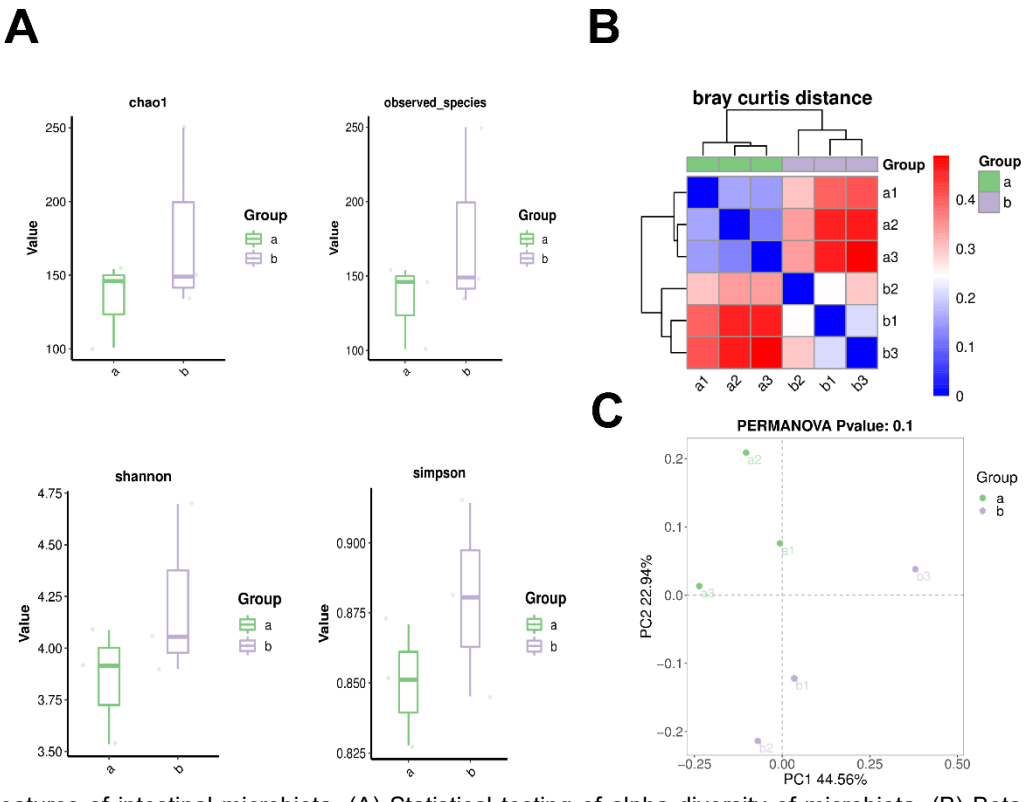

Fig. 7 Features of intestinal microbiota. (A) Statistical testing of alpha diversity of microbiota, (B) Beta diversity analysis of bacteria community, (C) Principal Component Analysis (PCA) of different samples

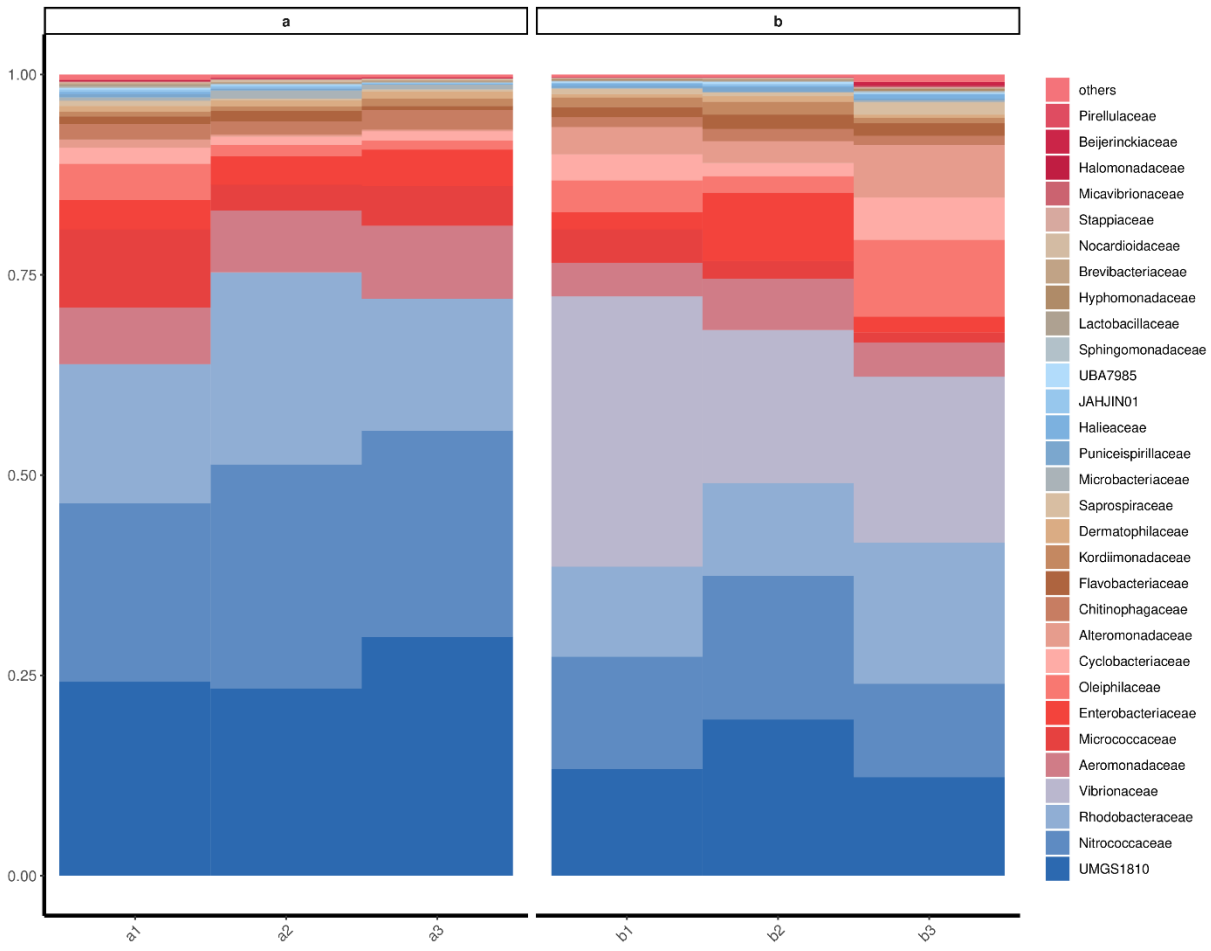

Fig. 8 Top 30 in relative abundance of intestinal microbiota

During pathogen exposure, the intestinal bacterial species of the control and experimental groups were further determined and compared (Fig. 8). At the phylum level, the dominant microflora of the two types of samples was *Bacteroidota* and *Actinomycetota*, the abundance of *Actinomycetota* in the control group was higher than that in the diseased samples, and the abundance of *Bacteroidota* in the experimental group was higher than that in the control group. The control group had high relative abundances of *Ascomycota*, *Planctomycetota*, *Verrucomicrobiota*, *Chloroflexota* and *Actinomycetota* while the experimental group had high relative abundances of *Bacteroidota*, *Pseudomonadota*, *Mucoromycota*. And the results were visualized by Croner (Fig. 9). At the genus level, *Vibrio* appeared in the experimental group, and the relative abundance of *Spiribacter*, *Aeromonas*, *Ruegeria* and *Rothia* decreased, and the relative abundance of *Vibrio Kordiimonas*, *Marinobacter*, *Alteromonas* increased.

LEfSe was uesd to identify key differential taxa in the gut microbiota (Fig. 10). The main biomarkers in the experimental group contained *Enterobacterales*, *Vibrio*, *Gammaproteobacteria*, and *Proteobacteria*. The main biomarkers in the control group contained *Nitrococcales* and *Clostridia*.

The t-test and Wilcoxon algorithm were used to analyze the significance of the difference between the two samples. The number of difference species was 33, difference genus was 18, and difference phylum was 4. Heatmap were made based on the relative abundance of differential species (Fig. 11A). *Gammaproteobacteria*, *Enterobacterales* increased with the exposure to the pathogen, and other classes such as *Cl.*, *Planctomycetia*, and *Verrucomicrobiae* decreased with the exposure to the pathogen. Correlations among microbial species and between species and environmental factors were assessed by Correlation heatmap analysis (Fig. 11B), among which the *Ruegeria*_B, *Spiribacter*, *NSJ_50*, *Aeromonas*, and *Agilicoccus* were significantly associated with *Vibrio*, showing reduced abundance during *Vibrio* dominance.

PICRUSt software was used to identify the KEGG function of the intestinal microbiota. We selected 36 significantly different metabolically relevant pathways at the level 2 of KEGG (Fig. 12A), among which strain infection significantly increased the majority of pathways of intestinal microbiota *V. parahaemolyticus* (amino acids and carbohydrate metabolism), and only Carotenoid biosynthesis,

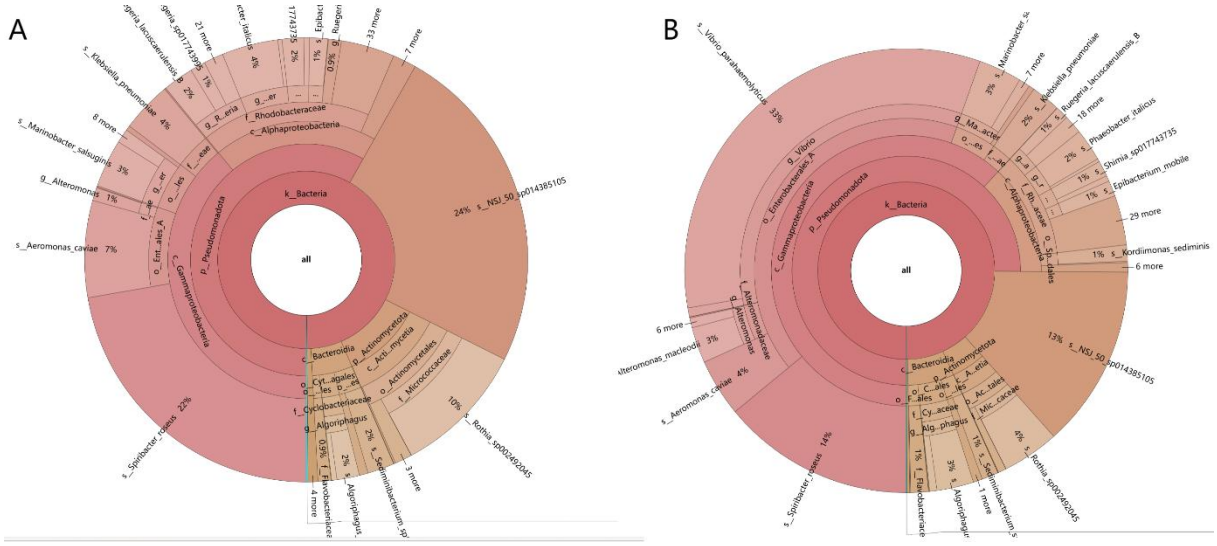

Fig. 9 Community structure krona analysis. (A) control group, (B) experimental group

Cocaine addiction, D-arginine, D-ornithine metabolism, Dopaminergic synapse, Isoflavonoid biosynthesis decreased at level 3 (Fig. 12B).

Discussion

In the past decade, *Vibrio*-related diseases, particularly acute hepatopancreatic necrosis disease (AHPND) and TPD, have severely impacted global shrimp farming (Yong *et al*., 2017). TPD primarily affects shrimp aged 6-12 d, with a mortality rate reaching up to 90% within 24 h of infection. We isolated a bacterial strain from the diseased shrimp, which could make shrimp produce TPD, and interestingly the strain could infect not only juvenile shrimps, but also adult shrimps. We identified that the strain is *V. parahaemolyticus*. The strain carries the TLH gene, but no TDH, TRH, *pir*A, *pir*B genes were detected. However, it carries the VHVP virulence factor, indicating the complexity of its pathogenic mechanisms (Li *et al*., 2019).

Bolitas syndrome is a larval syndrome of *P. vannamei* in which the symptoms are the isolation of epithelial cells from the intestine and hepatopancreas,

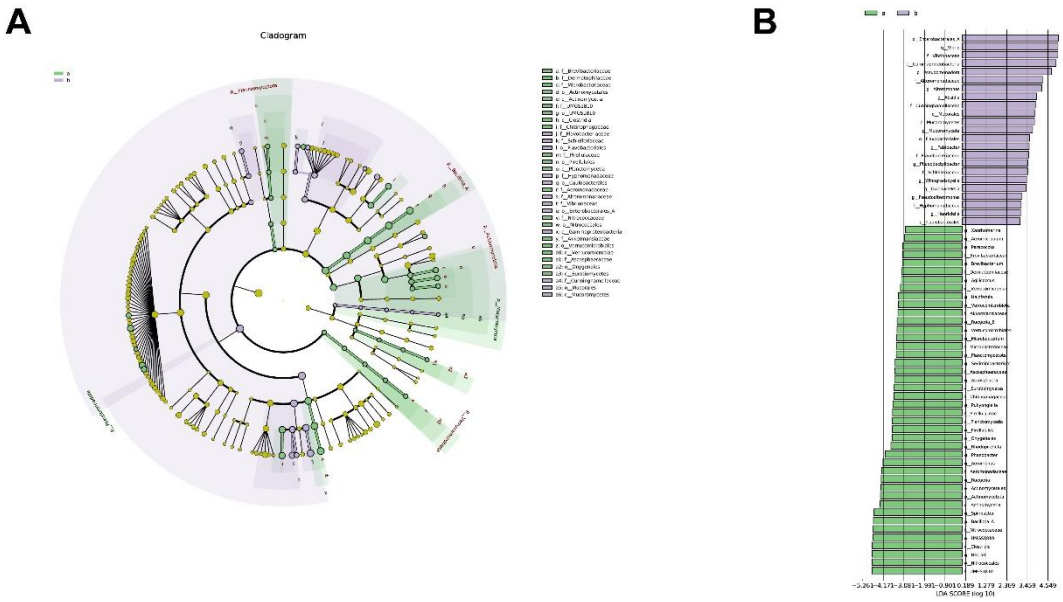

Fig. 10 Difference analysis of dominant taxa. (A) LEfSe multi-level species hierarchical cladogram map showing the phylogenetic distribution of bacterial lineages in different habitats, (B) Linear discriminant analysis showed indicator bacteria in different habitats

which appear as globular deposits in the digestive tract (Robertson *et al*., 1998). This was different from the histopathological state of the shrimps with TPD. The histologic lesions of the shrimps with TPD included severe hepatopancreatic epithelial cells shedding, tubules disruption, and irregular hepatopancreas contours (Yang *et al*., 2022).

However, the midgut structure was also destroyed in TPD, which was not the case in the AHPND. In this study, we found that there was a large number of bacterial colonization in the intestines, indicating that the intestinal flora and intestinal wall have been destroyed, and there will be a lot of black spots in the shrimp, which are rarely seen in past literature.

In recent years, major aquaculture countries worldwide have predominantly used antibiotics such as sulfamethoxazole, erythromycin, and amoxicillin (Lulijwa *et al*., 2020). However, the extensive use of antibiotics, combined with the hydrophilic and lipophilic characteristics of certain antibiotics, has led to a rapid increase in bacterial resistance (Sodhi *et al*., 2021). Antibiotic treatment recommendations for *V. parahaemolyticus* infections typically include tetracycline, fluoroquinolones, third-generation cephalosporins, aminoglycosides, and folate pathway inhibitors (Shaw *et al*., 2014). Notably, in our disk diffusion assay, the isolated bacteria were sensitive to ciprofloxacin, trimethoprim-sulfamethoxazole, and ceftriaxone, but exhibited resistance to tetracycline. These results highlighted the importance of selecting appropriate antibiotics in clinical treatment and provided a basis for further research.

The intestinal microbiota plays an important role in maintaining host health (Rooks and Garrett, 2016), Overall, changes in the intestinal bacterial community of shrimp were closely related to the severity and staging of the disease (Xiong *et al*., 2017). In this study, the increase in the alpha-diversity index indicated that the invasion of the strain would lead to the destruction of the shrimp intestine, allowing colonies in the environment to enter the intestine. Beta-diversity index showed that there were significant differences in the composition of intestinal microbiota community. The dominant classes in the shrimp gut were *Cl*., *Alphaproteobacteria*. *Proteobacteria* was the most abundant phylum in the gut of healthy and diseased *P. vannamei*. *Proteobacteria* are a symbiotic microbial community, and some members of this group have been reported to be opportunistic pathogens in marine animals, which could lead to dysbiosis of the gut microbiota (Holt *et al*., 2021). In this report, *V. parahaemolyticus* infection caused changes in the number of *Proteobacteria*, which led to a disturbance of intestinal absorption. Furthermore, substantial enrichment of *Alteromonas*, *Pseudomonas* and *Vibrio* were found in the intestines of diseased shrimp. These opportunistic pathogens showed a high degree of co-occurrence with the disease outbreak, indicating that ecological imbalance may have occurred in the shrimp gut, with a gradual shift from beneficial bacteria dominance to potential pathogens dominance, thereby exacerbating the symptoms of diseased shrimps.

The presence of the genera *L.* and *S.* is often associated with diseases of aquatic animals (Avendaño-Herrera *et al*., 2006). In the present study, the abundance of these genera increased after infection. *L.* and *S.* were negatively correlated with metabolites such as L-lysine, N6-acetyl-L-lysine and arginine-succinic acid, which were involved in lysine and arginine biosynthesis (Zhang *et al*., 2021). The increase in these genera may lead to a decrease in the levels of the essential amino acid lysine and arginine for shrimp (Li *et al*., 2025). In addition, the increased abundance of *L.* may disrupt the metabolism of purines and pyrimidines, leading to nucleotides deficiency and subsequent impairments in shrimp growth and immunity (Sauer *et al*., 2010).

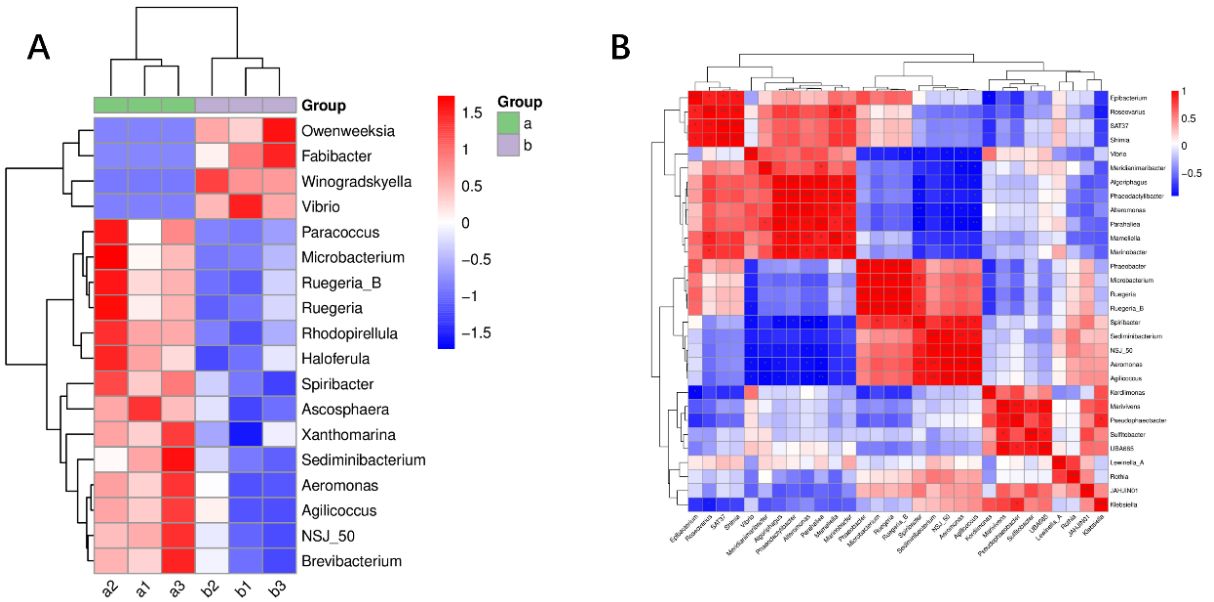

Fig. 11 Heatmap of differences in bacterial composition. (A) The genus level, (B) The species level

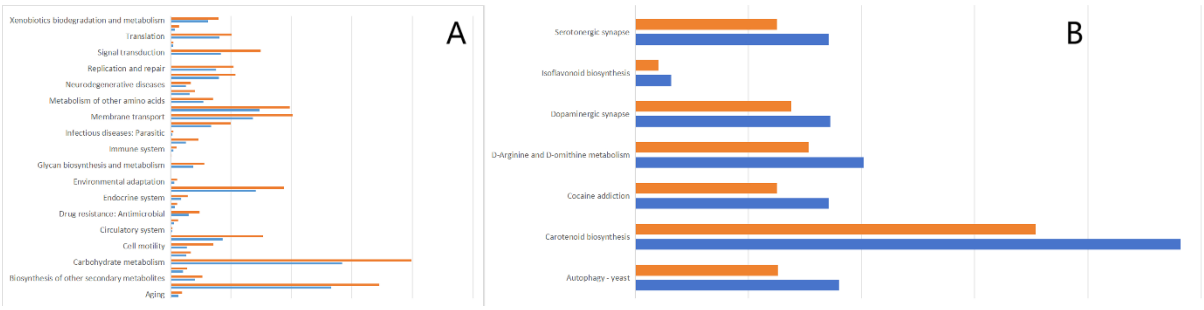

Fig. 12 Analysis of relative abundance of predicted functions at KEGG. (A) Level 2, (B) Level 3; orange: healthy shrimps, blue: diseased shrimps

L. also had the ability to use nucleotides as an energy source, which reduced nucleotide levels in the shrimp's gut (Khan *et al*., 2007).

Moreover, it was found that the differences of bacterial community functions between healthy and diseased shrimps were mainly reflected in auto metabolism, environmental information recognition and processing, and immune-related pathways. Based on the analysis of KEGG pathway database, the abundance of pathways related to carbohydrate metabolism in shrimp gut increased significantly after the invasion of pathogenic bacteria, indicating that the metabolic pattern of intestinal microbiota changed after the occurrence of disease. It was shown that carbohydrate metabolism was the main source of energy for bacteria during processes such as growth, virulence factor production, and colonization in hosts (Van Alst and Dirita, 2020). Thus, the increase in carbohydrate metabolism pathways favored host infection by *Vibrio*. Pathways related to the identification and processing of intestinal environmental information in sick shrimp have also been significantly increased, including two-component systems and membrane transport, which have been shown to regulate pathogen secretion and transmembrane transport (Jiang *et al*., 2026). In addition, significant up-regulation of genes closely related to bacterial pathogenicity, such as homologous recombination and flagellar assembly, was also observed in shrimp gut (Yu *et al*., 2022). In the immune system, arginine has been chosen as a node for regulating the immune response, and arginine, in addition to being a component of protein synthesis, was a substrate that profoundly influences the biology of immune cells, especially macrophages. Its fine-tuning could determine different pro-inflammatory or anti-inflammatory immune results. In the level 3, there was a significant decrease in endocytosis, indicating that the immune system of shrimp was disrupted, and the significant decrease in D-arginine and D-ornithine pathways also corroborated this conclusion from biosynthesis.

Conclusion

This study delved into the *V. parahaemolyticus* H1, which was capable of infecting both juvenile and adult shrimp. Through a series of experiments, including samples collection from diseased shrimps, bacterial isolation and identification, virulence factors screening, physiological and biochemical analysis, antibiotic resistance testing, and histopathological examination, the pathogenic characteristics of *V. parahaemolyticus* H1 and its effects on shrimp were also systematically explored. The study revealed the complex impact of *V. parahaemolyticus* H1 infection on shrimp, demonstrating that the bacterium not only damaged the host's physiological functions but also significantly disrupted the intestinal microbiota, leading to dysbiosis.

Acknowledgements

This work was supported by the Science and Technology Talent Innovation Project of Hainan Province (KJRC2025B14), the Innovation Capacity Enhancement Project of Hebei Province (253A6701D), and the China Agriculture Research System of MOF and MARA (CARS-49).

References

Ashrafudoulla M, Na KW, Hossain MI, Mizan MFR, Nahar S, Toushik SH, *et al*. Molecular and pathogenic characterization of *Vibrio parahaemolyticus* isolated from seafood. Mar. Pollut. Bull. 172: 112927, 2021.

Avendaño-Herrera R, Toranzo AE, Magariños B. Tenacibaculosis infection in marine fish caused by Tenacibaculum maritimum: a review. Dis. Aquat. Organ. 71: 255-266, 2006.

Avershina E, Frisli T, Rudi K. *De novo* semi-alignment of 16S rRNA gene sequences for deep phylogenetic characterization of next generation sequencing data. Microbes Environ. 28(2): 211-216, 2013.

Broberg CA, Calder TJ, Orth K. *Vibrio parahaemolyticus* cell biology and pathogenicity determinants. Microbes Infect. 13(12-13): 992-1001, 2011.

Caporaso JG, Kuczynski J, Stombaugh J, Bittinger K, Bushman FD, Costello EK, *et al*. QIIME allows analysis of high-throughput community sequencing data. Nat. Methods. 7(5): 335-336, 2010.

Darshanee Ruwandeepika HA, Sanjeewa Prasad Jayaweera T, Paban Bhowmick P, Karunasagar I, Bossier P, Defoirdt T. Pathogenesis, virulence

factors and virulence regulation of vibrios belonging to the *Harveyi clade*. Rev. Aquacult. 4(2): 59-74, 2012.

Han L, Yan P, Wang M. Comparative analysis on survival and tissue damage of different environmental stress factors in Pacific white shrimp *Litopenaeus vannamei*. Comp. Immunol. Rep. 8: 200219, 2025.

Hu F, Wang S, Hu J, Bao Z, Wang M. Comprehensive evaluation of dietary tandem CpG oligodeoxynucleotides on enhancement of antioxidant capacity, immunological parameters, and intestinal microbiota in white shrimp (*Litopenaeus vannamei*). Aquaculture. 579: 740250, 2024.

Holt CC, Bass D, Stentiford GD, van der Giezen M. Understanding the role of the shrimp gut microbiome in health and disease. J. Invertebr. Pathol. 186: 107387, 2021.

Jia X, Tao Y, Shi B, Liu J, Qin J, Zhang L, *et al*. Development and application of SYBR Green-based qPCR method to detect *Vibrio parahaemolyticus* causing translucent post-larvae disease in shrimp *Litopenaeus vannamei*. J. Invertebr. Pathol. 214: 108475, 2026.

Jiang L, Wang M, Guo Y. Proteomic analysis of the hepatopancreas in *Litopenaeus vannamei* artificially infected by *Vibrio parahaemolyticus* causing acute hepatopancreatic necrosis disease. Aquaculture. 614: 743541, 2026.

Khan ST, Fukunaga Y, Nakagawa Y, Harayama S. Emended descriptions of the genus *Lewinella* and of *Lewinella cohaerens*, *Lewinella nigricans* and *Lewinella persica*, and description of *Lewinella lutea* sp. nov. and *Lewinella marina* sp. nov. Int. J. Syst. Evol. Microbiol. 57(12): 2946-2951, 2007.

Li H, Zhang L, Chen T, Hou Y, Yan P, Zeng Q, *et al*. The discovery of disease resistance-related factors based on exoskeleton components in the Pacific white shrimp *Litopenaeus vannamei*. Dev. Comp. Immunol. 170: 105431, 2025.

Li L, Meng H, Gu D, Li Y, Jia M. Molecular mechanisms of *Vibrio parahaemolyticus* pathogenesis. Microbiol. Res. 222: 43-51, 2019.

Lulijwa R, Rupia EJ, Alfaro AC. Antibiotic use in aquaculture, policies and regulation, health and environmental risks: a review of the top 15 major producers. Rev. Aquacult. 12(2): 640-663, 2020.

Mahoney JC, Gerding MJ, Jones SH, Whistler CA. Comparison of the pathogenic potentials of environmental and clinical *Vibrio parahaemolyticus* strains indicates a role for temperature regulation in virulence. Appl. Environ. Microb. 76(22): 7459-7465, 2010.

Ni P, Ma Y, Shi B, Wang M. Histopathological and proteomics analysis of shrimp *Litopenaeus vannamei* infected with *Ecytonucleospora hepatopenaei*. Microorganisms, 13(2): 402, 2025.

Robertson PAW, Calderon J, Carrera L, Stark JR, Zherdmant M, Austin B. Experimental *Vibrio harveyi* infections in *Penaeus vannamei* larvae. Dis. Aquat. Organ. 32(2): 151-155, 1998.

Rooks MG, Garrett WS. Gut microbiota, metabolites and host immunity. Nat. Rev. Immunol. 16(6): 341-352, 2016.

Sauer N, Bauer E, Vahjen W, Zentek J, Mosenthin R. Nucleotides modify growth of selected intestinal bacteria *in vitro*. Livest. Sci. 133(1-3): 161-163, 2010.

Schloss PD, Westcott SL, Ryabin T, Hall JR, Hartmann M, Hollister EB, *et al*. Introducing mothur: open-source, platform-independent, community-supported software for describing and comparing microbial communities. Appl. Environ. Microb. 75(23): 7537-7541, 2009.

Shaw KS, Rosenberg Goldstein RE, He X, Jacobs JM, Crump BC, Sapkota AR. Antimicrobial susceptibility of *Vibrio vulnificus* and *Vibrio parahaemolyticus* recovered from recreational and commercial areas of Chesapeake Bay and Maryland Coastal Bays. PloS ONE. 9(2): e89616, 2014.

Shi B, Zhang L, Jia X, Tao Y, Wang M. Profiles of gut microbiome in *Litopenaeus vannamei* artificially infected with *Vibrio parahaemolyticus* causing translucent post-larva disease. Dev. Comp. Immunol, 176: 105565, 2026.

Sodhi KK, Kumar M, Singh DK. Insight into the amoxicillin resistance, ecotoxicity, and remediation strategies. J. Water Process Eng. 39: 101858, 2021.

Sun J, Wang Y, Hu F, Hu JJ, Wang MQ. Comparative study of two novel extracellular copper/zinc superoxide dismutase (Cu-Zn SOD) genes from white shrimp *Litopenaeus vannamei*. ISJ-Invert. Surv. J. 19: 126-135, 2022.

Van Alst AJ, Dirita VJ. Aerobic metabolism in *Vibrio cholerae* is required for population expansion during infection. MBio. 11(5): 10-1128, 2020.

Wang GZ, Wang YX, Wang MQ. Influence of sex on intestinal microbiota of Pacific white shrimp *Penaeus vannamei*. ISJ-Invert. Surv. J. 22: 49-56, 2025.

Wang L, Gong X, Chen G, Hu F, Wang M. The immunomodulation of *Synechococcus elongatus* PCC7942 carrying a tandem CpG oligodeoxynucleotides in Pacific white shrimp *Litopenaeus vannamei*. Aquaculture. 614: 743569, 2025.

Xiong J, Zhu J, Dai W, Dong C, Qiu Q, Li C. Integrating gut microbiota immaturity and disease-discriminatory taxa to diagnose the initiation and severity of shrimp disease. Environ. Microbiol. 19(4): 1490-1501, 2017.

Yang F, Xu L, Huang W, Li F. Highly lethal *Vibrio parahaemolyticus* strains cause acute mortality in *Penaeus vannamei* post-larvae. Aquaculture. 548: 737605, 2022.

Yong CY, Yeap SK, Omar AR, Tan WS. Advances in the study of nodavirus. PeerJ. 5: e3841, 2017.

Yu P, Shan H, Cheng Y, Ma J, Wang K, Li H. Translucent disease outbreak in *Penaeus vannamei* post-larva accompanies the imbalance of pond water and shrimp gut microbiota homeostasis. Aquacult. Rep. 27: 101410, 2022.

Zhang X, Sun J, Han Z, Chen F, Lv A, Hu X, *et al*. *Vibrio parahaemolyticus* alters the community composition and function of intestinal microbiota in Pacific white shrimp, *Penaeus vannamei*. Aquaculture. 544: 737061, 2021.

Zhong X, Pan Z, Mu Y, Zhu Y, Zhang Y, Ma J, *et al*. Characterization and epidemiological analysis of *Vibrio parahaemolyticus* isolated from different marine products in East China. Int. J. Food Microbiol. 380: 109867, 2022.

Zou Y, Xie G, Jia T, Xu T, Wang C, Wan X, *et al*. Determination of the infectious agent of translucent post-larva disease (TPD) in *Penaeus vannamei*. Pathogens. 9(9): 741, 2020.